# A Fully Polarimetric Meteor Radar

## John Marino, Nicholas Rainville, and Scott E. Palo

Abstract – This study presents initial results from a fully polarimetric meteor radar, in which a complete scattering matrix is constructed at each time step of observation. Findings highlight the temporal evolution of scattering mechanisms within meteor echoes. The study underscores the potential benefits of integrating polarimetric capability into meteor radar systems, opening a path for further investigations into radio meteor behavior and enhancing the scientific value of meteor radar data.

#### 1. Introduction

Meteor radars play a significant role in studying meteoroids and the upper atmosphere by observing reflected radio frequency (RF) energy scattered from plasma trails during a meteor's entry into the atmosphere. Many installations, whether traditional monostatic systems or newer multistatic systems, use a single polarization during transmission and reception, which is often circular. Circular polarization, being less sensitive to target orientation, mitigates polarization losses given the uncertainty around the exact linear orientation of a meteor's trail within the reflection plane. Currently, this status quo has been a reasonable compromise between system complexity and information collected, particularly in commercial systems whose core science product of hourly winds in the mesosphere and lower thermosphere need only the echo spatial location and body Doppler shift to infer wind velocity.

The earliest studies concerning the radio propagation of meteors predicted differences in polarization behavior [1]. Even in the early experimental stages concurrent with the formulation of the classical model, some experiments explored the polarization response of echoes in the context of plasma resonance [2, 3]. However, since then, and even through the introduction of modern digital meteor radar technology in the early 2000s, the prevailing use of single-polarization in commercial meteor radar systems has endured.

When studying meteor burst communications, Wei et al. [4] framed older experiments [2, 3] regarding

Manuscript received 18 December 2023. This work was supported by National Science Foundation (NSF) award AGS-1933007 as part of the as part of the Distributed Array of Small Instruments (DASI) program (NSF-545) and award OPP-1543446 for the meteor radar at McMurdo Station Antarctica.

John Marino, Nicholas Rainville, Scott E. Palo, are with the Ann & H.J. Smead Department of Aerospace Engineering Sciences, University of Colorado Boulder College of Engineering and Applied Science, 3775 Discovery Drive, 29 UCB Boulder, Colorado, 80309, USA; e-mail: john.marino@colorado.edu, nicholas.rainville@colorado.edu, palo@colorado.edu.

the polarization scattering matrix. Also, studying meteor burst communications, Chung [5] made multifrequency orthogonal polarization measurements with a forward scatter very high-frequency radar. More recent experiments with meteor trail polarization include Close et al., [6] who examined the scattering and polarization of a long meteor trail using the Advanced Research Project Agency (ARPA) Long-Range Tracking and Identification Radar (ALTAIR), and Stober et al. [7] who examined reflection coefficients with the Southern Argentina Agile MEteor Radar Orbital System (SAAMER-OS).

In this work, we introduce the concept of fully polarimetric meteor radar, in which a complete scattering matrix is constructed at every time step of observation, providing a complete description of the meteor scatterer at the probing frequency and aspect angle. A prototype implementation with the Zephyr Meteor Radar Network [8] using simultaneously transmitting and receiving orthogonal linear polarizations with a coded continuous wave technique is described in Section 4.

Radar polarimetry can provide a comprehensive description of the properties of a radar scatterer. When applied to meteor radar, it has the potential to improve detection and enable more accurate discrimination. It can also enhance understanding of the physical characteristics of plasma trails, which can lead to new insights and increase the scientific value of meteor radar data.

#### 2. The Scattering Matrix

The scattering matrix,  $\overline{\overline{S}}$ , is a mathematical description of a target's response to an electromagnetic wave. It represents the target as a polarization transformer and links the Jones vectors of incident,  $\overline{E}_i$ , and scattered,  $\overline{E}_s$ , waves,

$$\begin{bmatrix}
E_{H}^{s} \\
E_{V}^{s}
\end{bmatrix} = \frac{e^{-jkr}}{r} \begin{bmatrix}
S_{HH}(\hat{k}_{i}, \hat{k}_{s}) & S_{HV}(\hat{k}_{i}, \hat{k}_{s}) \\
S_{VH}(\hat{k}_{i}, \hat{k}_{s}) & S_{VV}(\hat{k}_{i}, \hat{k}_{s})
\end{bmatrix} \begin{bmatrix}
E_{H}^{i} \\
E_{V}^{i}
\end{bmatrix} . (1)$$
For pagation term
$$\begin{bmatrix}
S_{HH}(\hat{k}_{i}, \hat{k}_{s}) & S_{HV}(\hat{k}_{i}, \hat{k}_{s}) \\
S_{VV}(\hat{k}_{i}, \hat{k}_{s})
\end{bmatrix} \underbrace{E_{H}^{i} \\
E_{V}^{i}
\end{bmatrix} . (1)$$

The scattering matrix depends on the frequency,  $f_0$ , and direction,  $k_i$ , of the incident wave, and the direction of the scattered wave,  $k_s$ , often thought of in terms of a forward scattering angle,  $2\phi$ , as seen in the left panel of Figure 1.

The elements of the Jones vector and scattering matrix in (1) are given in terms of linear horizontal (H) and vertical (V) polarization, for example, but any orthogonal basis will suffice, such as left-handed circular and right-handed circular polarization. Unlike the

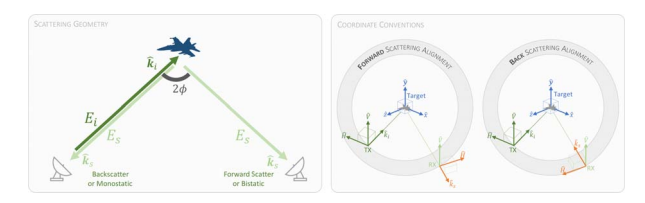


Figure 1. (Left) Sketch of scattering geometry showing bistatic angle. (Right) Illustration of back and forward scatter coordinate conventions.

monostatic case, in the case of forward-scatter, the diagonal elements are not equal,  $S_{HH} \neq S_{VV}$ .

## 3. Radar Polarimetry

Polarimetry is a measurement technique in remote sensing that uses the polarized nature of electromagnetic radiation to derive information about the physical properties of a scattering target, including size, shape, orientation, and composition. It is regularly used in weather radar applications to estimate the amount of precipitation in a volume, to distinguish between different types of precipitation, such as rain, hail, and snow, to deduce physical properties, such as drop size distribution, and to discriminate between meteorological and nonmeteorological targets [9]. This technology is so useful for meteorology and weather forecasting that the National Weather Service upgraded its national nextgeneration radar (Nexrad) network of Doppler Weather Surveillance Radars with polarimetric capability in 2011 [10]. Polarimetry is also regularly employed in airborne and space-based synthetic aperture radar (SAR) imaging applications, such as vegetation mapping [11], flood mapping [12], geohazard monitoring [13], urban mapping [14], agricultural monitoring [15], ship detection [16], and others.

### 4. A Polarimetric Meteor Radar

The Zephyr Meteor Radar Network is a prototype meteor radar system in development along Colorado's Front Range. At the time of data collection, the network consisted of a single interferometric transmitting station in Platteville, CO, and three receivers deployed some tens of kilometers away in a forward scatter configuration. It operates at 31.250 MHz and transmits 500 W with continuous modulation from each of the six transmit channels (north, south, east, west, center A, center B).

The radar system employs a continuous wave code division multiple access transmission scheme as detailed by [17]. This scheme allows multiple colocated transmitters to operate within the same frequency band by sending unique orthogonal codes. The Zephyr system uses a traditional asymmetric cross-array with circularly polarized elements for calibrated direction-finding interferometry [18], as shown in Figure 2. Dual-orthogonal polarizations are achieved by transmitting separate codes to each of two orthogonal linearly polarized antenna elements of the central antenna.

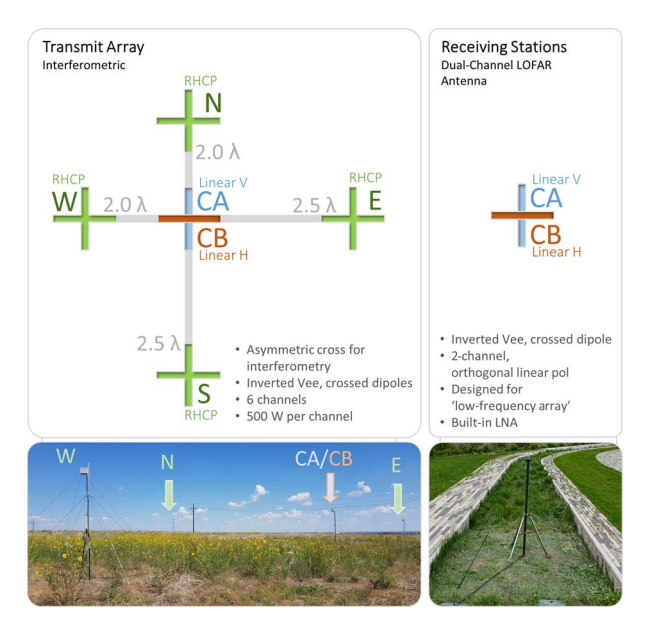


Figure 2. Diagram of the transmit array and typical receiving antenna.

At the receiving stations, both polarizations are simultaneously digitized after reception from a single, dual-polarized, crossed-dipole antenna in an inverted-V configuration, as shown in Figure 2. By correlating a template of the two codes sent through the linear-H and linear-V transmit antenna elements with the two data streams received through the linear-H and linear-V receive antenna, a complex scattering matrix is constructed at each time step of observation, as illustrated in Figure 3. This approach diverges from that of typical polarimetric radars, where pulses alternate of alternating polarization are used to construct a scattering matrix. The application is also unique in that it has not been previously applied to an all-sky meteor radar.

## 5. Results

The dataset for this study comprises approximately 235,000 echoes recorded between January 2023 and June 2023 from the Platteville, CO (TX)–Parker, CO (RX) link, having a separation baseline of 72 km. Each echo consists of four complex in-phase (I) and quadrature (Q) time series in the 4 s surrounding a detection event, representing the elements of the scattering matrix,  $\overline{S}$ . These are a subset of the full 12 time series resulting from the correlation of six transmit channel codes with the data streams from two receiving channels. For each echo, the bistatic range is recorded, a Doppler shift and associated velocity along the bisector vector is computed, as well as the echo's spatial location (both azimuth and elevation and latitude, longitude, altitude).

Figure 3 shows the time evolution of typical meteor echoes collected on the system. Each represents 4 s of IQ data around an event at a particular range gate,

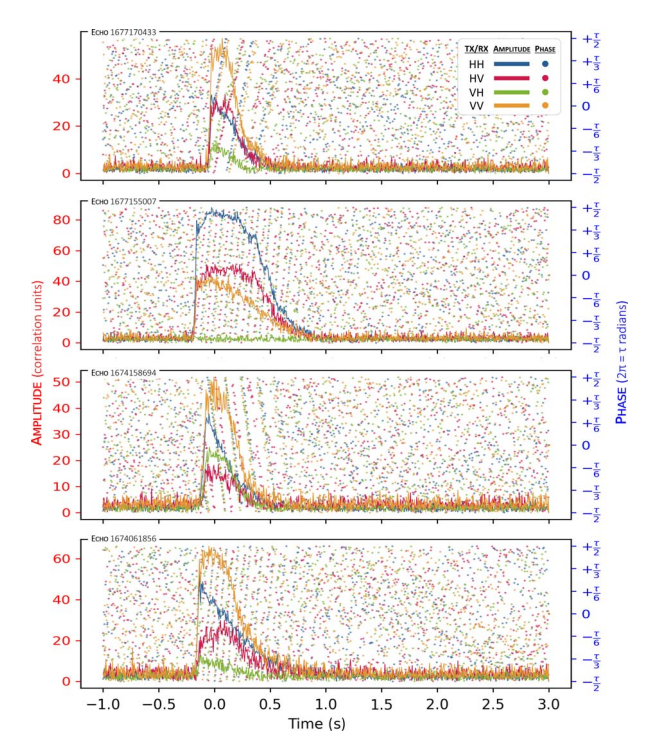


Figure 3. Several examples of typical polarimetric meteor echo signatures are recorded on the Zephyr Meteor Radar Network. Each trace represents an element of the scattering matrix (HH, HV, VH, VV) in amplitude and phase.

shown as amplitude (solid line) and phase (circle points). The four elements of the scattering matrix are shown as follows: HH, HV, VH, and VV.

Note the shifting contributions of scattering components in the time series, which confirm that the target's underlying physical characteristics are evolving over time. While it is beyond the scope of this letter to interpret the physical mechanisms driving the polarization signature, these examples highlight the dynamic nature of the observations in the data set. The novel aspects revealed in this study emphasize the need for further in-depth investigation.

Examining the data set as a whole, Figure 4 shows histograms of the amplitude contributions of each scattering matrix component around " $t_0$ ," that is approximately around the time of peak echo amplitude, just after trail formation. The copolarization components (HH and VV) contribute most greatly to the scattering matrix in this data set.

One way to begin to unravel the data set is to perform a polarimetric decomposition, as is common in SAR data analysis. It is possible to decompose a scattering matrix into components with a physical interpretation. The components can be used to discern useful information about the size, shape, orientation, and composition of the target. A canonical example, although certainly not the only or most robust example, is the Pauli decomposition, which refactors the scattering matrix into a summation of orthogonal bases whose

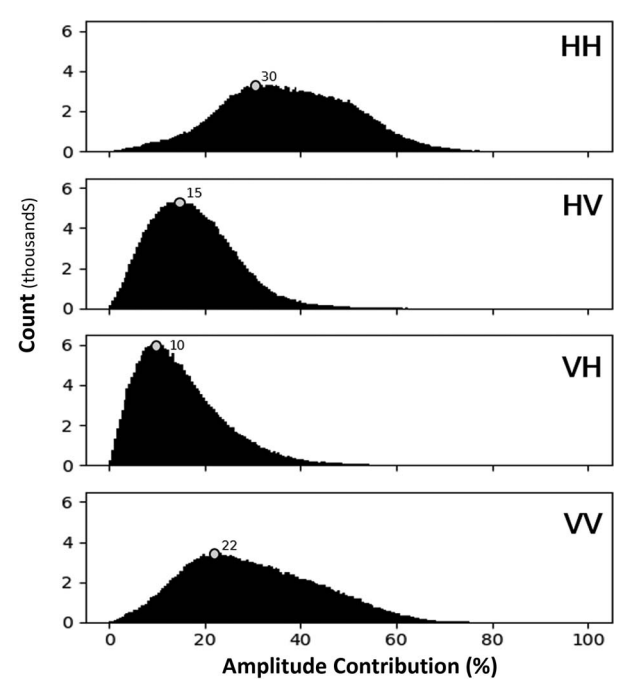


Figure 4. Histograms counting the amplitude contribution of each element in the scattering matrix for the echoes in the dataset.

complex coefficients indicate the degree of contribution of various canonical scattering mechanisms [19],

$$\overline{\overline{S}} = \begin{bmatrix} a+b & c-jd \\ c+jd & a-b \end{bmatrix}$$
 (2)

$$a = \frac{1}{2}(S_{HH} + S_{VV})$$
 Spheres, cylinders, trihedrals, planes
(3)

$$b = \frac{1}{2}(S_{HH} - S_{VV})$$
 Dihedrals with 0° line-of-  
sight rotation (4)

$$c = \frac{1}{2}(S_{HV} + S_{VH})$$
 Dihedrals with 45° line-of-  
sight rotation (5)

$$d = \frac{1}{2}(S_{HV} - S_{VH}) \text{ Helicity}$$
 (6)

$$\overline{\overline{S}} = a \begin{bmatrix} 1 & 0 \\ 0 & 1 \end{bmatrix} + b \begin{bmatrix} 1 & 0 \\ 0 & -1 \end{bmatrix} + c \begin{bmatrix} 0 & 1 \\ 1 & 0 \end{bmatrix} + d \begin{bmatrix} 0 & -j \\ j & 0 \end{bmatrix}.$$
(7)

In Figure 5, the normalized amplitudes of the Pauli coefficients for the meteors shown in Figure 3 are represented as stacked gradient charts to help compare

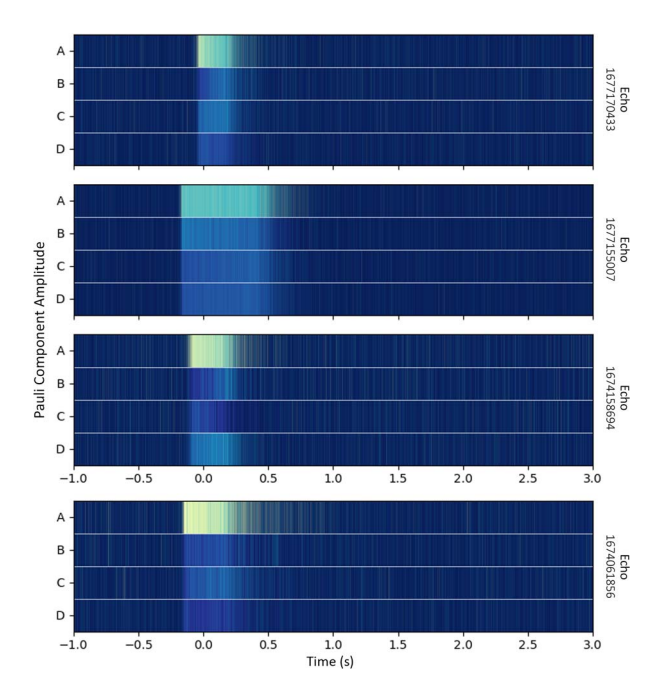


Figure 5. Normalized components of the Pauli Decomposition for each echo are shown in Figure 3. Brighter shades indicate a higher responsiveness to a particular component.

components. Not surprisingly, for specular meteor reflections, the dominant component is the "Pauli A: single-bounce" coefficient, which indicates the responsiveness of spherical, cylindrical, planar, and trihedral targets. Even so, the contributions of other components vary, once again highlighting that the target's underlying physical characteristics are evolving over time.

#### 6. Alignment

Future efforts will explore a complete polarimetric calibration [20]. For this study, antenna alignment and channel imbalance were addressed as follows. Antenna elements were aligned to the cardinal directions as follows: north and south for the "vertical" polarization antennas, and east and west for the "horizontal" polarization antennas. In case of misalignment, it is possible to rotate the scattering matrix to reorient the polarimetric bases,

$$\mathbf{S}' = \begin{bmatrix} \cos(-\theta_R) & -\sin(-\theta_R) \\ \sin(-\theta_R) & \cos(-\theta_R) \end{bmatrix} \begin{bmatrix} S_{11} & S_{12} \\ S_{21} & S_{22} \end{bmatrix} \\ \begin{bmatrix} \cos(\theta_T) & -\sin(\theta_T) \\ \sin(\theta_T) & \cos(\theta_T) \end{bmatrix}, \tag{8}$$

where  $\theta_R$  and  $\theta_T$  are the counterclockwise rotations from the horizontal "H" direction in the receiver and transmitter reference planes.

Care must also be taken to ensure that each transmitting channel radiates with equal power amplitude and phase and that each receiving channel is equally responsive to an identical input signal in amplitude and

phase. Each receiver channel must be characterized such that a correction can be applied if necessary; for example,

$$H_{RX}' = Ae^{i\phi} \times H_{RX} \tag{9}$$

$$V_{RX}' = V_{RX}. \tag{10}$$

#### 7. Conclusions and Future Work

This study presents preliminary findings from the inaugural deployment of a fully polarimetric meteor radar. It illuminates the temporal evolution of scattering mechanisms within meteor echoes and their detectability by polarimetric signature. These distinctive features open novel avenues for investigating the behavior of radio meteor echoes, offering new insights and enhancing the scientific value of meteor radar data.

Contemporary meteor radar systems overwhelmingly employ interferometric direction-finding arrays, with an emerging trend of incorporating continuous wave-code division multiple-access transmission schemes. Integrating orthogonal polarizations by adding or reconfiguring two-transmit channels is readily achievable. Similarly, the widespread use of multichannel, software-defined radio receivers supports orthogonal polarizations on the receiving side with minimal additional cost.

The potential benefits that could result from the marginal expenses associated with outfitting a radar system for polarimetry are compelling. Possible use cases include decompositions that maximize signal-to-noise ratio for enhanced detection, introduction of polarimetric criteria for target discrimination, estimation of the meteor trail's spatial orientation within its reflection plane, calibration opportunities with aircraft signatures, and a reframing of the full-wave model in terms of the scattering matrix, along with an extension of the classical underdense radio meteor model to include polarization effects.

#### 8. References

- T. R. Kaiser, and R. L. Closs, "Theory of Radio Reflections from Meteor Trails," *The London, Edinburgh, and Dublin Philosophical Magazine and Journal of Science*, 43, 336, October 1952. pp. 1–32.
- E. R. Billam, I. C. Browne, "Characteristics of Radio Echoes from Meteor Trails IV: Polarization Effects," *Proceedings of the Physical Society*. Section B. 69, 1, 1956, p. 98.
- M. E. van Valkenburg, "The Two-Helix Method for Polarization Measurement of Meteoric Radio Echoes," *Journal of Geophysical Research* (1896–1977), 59, 3 September 1954, pp. 359–364, doi: 10.1029/JZ059i003p00359.
- P. S. P. Wei, C. R. Miller, and C. K. Martin, "Polarization Effects in Radio Wave Scattering from Meteor Bursts," *IEEE Military Communications Conference, Bridging the Gap, Interoperability, Survivability, Security,* 2, October 1989, pp. 433–439, doi: 10.1109/milcom.1989.103967.
- S. Chung, A. R. Webster, K. J. Ellis, and J. Jones, "A comparison of Vertically and Horizontally Polarized Antennas

- for Meteor Burst Communication at Long Ranges," Seventh International Conference on HF Radio Systems and Techniques, Nottingham, UK, July 7–10, 1997, pp. 349–352, doi: 10.1049/cp:19970818.
- S. Close, M. Kelley, L. Vertatschitsch, P. Colestock, M. Oppenheim, et al., "Polarization and Scattering of a Long-Duration Meteor Trail," *Journal of Geophysical Research: Space Physics*, 116, A1, January 2011, doi: 10.1029/2010JA015968.
- G. Stober, R. Weryk, D. Janches, E. C. M. Dawkins, et al., "Polarization Dependency of Transverse Scattering and Collisional Coupling to the Ambient Atmosphere From Meteor Trails – Theory and Observations," *Planetary and Space Science* 237, 2023, p. 105768, doi: 10.1016/j.pss. 2023.105768.
- N. Rainville, J. Marino, S. E. Palo, and R. Volz, "Multistatic Radar Development for the Colorado Zephyr Meteor Radar Network," *URSI Radio Science Letters*, 4 2023.
- E. A. Brandes, G. Zhang, and J. Vivekanandan, "Drop Size Distribution Retrieval With Polarimetric Radar: Model and Application," *Journal of Applied Meteorology*, 43, 3, April 2004, pp. 461–475, doi: 10.1175/1520-0450(2004)043<0461: dsdrwp>2.0.co;2.
- R. J. Doviak, V. Bringi, A. Ryzhkov, A. Zahrai, and D. Zrnić, "Considerations for Polarimetric Upgrades to Operational WSR-88D Radars," *Journal of Atmospheric and Oceanic Technology*," 17, 3, 2000, pp. 257–278, doi: 10. 1175/1520-0426(2000)017<:cfputo>2.0.co;2.
- A. Freeman, and B. van den Broek, "Mapping Vegetation Types Using SIR-C Data," 1995 International Geoscience and Remote Sensing Symposium, IGARSS '95. Quantitative Remote Sensing for Science and Applications, Firenze, Italy, July 10–14, 1995, doi: 10.1109/IGARSS.1995.521097.
- 12. M.-J. Jo, B. Osmanoglu, B. Zhang, and S. Wdowinski, "Flood Extent Mapping Using Dual-polarimetric Sentinel-1 Synthetic Aperture Radar Imagery," *The Interna*tional Archives of the Photogrammetry, Remote Sensing

- and Spatial Information Sciences, XLII-3, 2018, pp. 711–713, doi: 10.5194/isprs-archives-XLII-3-711-2018.
- C. Wang, X. Mao, and Q. Wang, "Landslide Displacement Monitoring by a Fully Polarimetric SAR Offset Tracking Method," *Remote Sensing*, 8, 8, July 2016, pp. 1–20, doi: 10.3390/rs8080624.
- 14. S. Dey, N. Bhogapurapu, A. Bhattacharya, A. C. Frery, and P. Gamba, "Built-Up Area Mapping Using Full and Dual Polarimetric SAR Data," 2021 IEEE International Geoscience and Remote Sensing Symposium IGARSS, Brussels, Belgium, July 11–16, 2021, pp. 1693–1696, doi: 10.1109/igarss47720.2021.9553040.
- J. M. Lopez-Sanchez, and J. D. Ballester-Berman, "Potentials of Polarimetric SAR Interferometry for Agriculture Monitoring," *Radio Science*, 44, 2, March 2009, pp. 1–20, doi: 10.1029/2008rs004078.
- R. Touzi, F. J. Charbonneau, R. K. Hawkins, and P. W. Vachon, "Ship Detection and Characterization Using Polarimetric SAR," *Canadian Journal of Remote Sensing*, 30, 3, June 2004, pp. 552–559, doi: 10.5589/m04-002.
- J. Vierinen, J. L. Chau, N. Pfeffer, M. Clahsen, and G. Stober, "Coded Continuous Wave Meteor Radar," *Atmospheric Measurement Techniques*, 9, 2, March 2016, pp. 829–839.
- J. Marino, N. Rainville, J. Monaco, S. E. Palo, and R. Volz, "Meteor Radar Phase Interferometry Calibration with Aircraft Observations and ADS-B Integration," United States National Committee of URSI National Radio Science Meeting (USNC-URSI NRSM), Boulder, CO, USA, January 9– 13, 2024, pp. 35–36.
- C. López-Martínez, and E. Pottier. "Basic Principles of SAR Polarimetry," in: I. Hajnsek, Y. L. Desnos (eds), *Polar-imetric Synthetic Aperture Radar.*, vol 25. Cham, Springer, 2021, Chapter 1.
- A. Freeman, "SAR Calibration: An Overview," *IEEE Transactions on Geoscience and Remote Sensing*, 30 6, November 1992, pp. 1107–1121. doi: 10.1109/36.193786.